Component Segregation in Model Chemically Amplified Resists[*]

John T. Woodward[a], Theodore H. Fedynyshyn[b], David K. Astolfi[b], Susan Cann[b], Jeanette M. Roberts[c], Michael J. Leeson[c]

[a]Optical Technology Division, National Institute of Standards and Technology, Gaithersburg, MD 20899
[b]MIT Lincoln Laboratory, Lexington, MA 02420
[c]Intel Corporation, Hillsboro, OR 97124

ABSTRACT

We have applied chemical force microscopy (CFM) to probe the surface roughness of partially developed model resist materials in order to understand the fundamental materials properties of the resists leading to line edge roughness (LER). CFM is capable of providing simultaneous information about surface topography and chemical heterogeneity of partially developed resist films. We have used CFM to study ESCAP type resists that are used in 248 nm and extreme ultraviolet (EUV) lithography. We observe changes in both the innate material roughness and chemical heterogeneity of the resist with the introduction of photoacid generator (PAG) and with exposure and post exposure bake (PEB). We find several mechanisms by which chemical heterogeneity can contribute to increasing the innate material roughness of the resist.

Keywords: Photoresist, line edge roughness, PAG, atomic force microscopy, chemical force microscopy.

1. INTRODUCTION

The reduction of line edge roughness (LER) is one of the leading challenges to developing photoresists for advanced lithography in high volume manufacturing. As LER requirements head below 5 nm they become equivalent to the length scales of the fundamental properties of the resist such as polymer size and acid diffusion lengths. Thus the ability to control LER will depend on an understanding of the fundamental material properties and processes of the resist.

For extreme ultraviolet lithography (EUVL), the high cost of EUV photons dictates that chemically amplified resists will likely continue to be the paradigm of choice for advanced resists. ESCAP type resists that are widely used in 248 nm lithography have optical properties that are compatible with EUVL making them leading candidates for advanced resists. We therefore have chosen ESCAP type resists consisting of hydroxystyrene (HOST), styrene, and tert-butyl acrylate (TBA) co-polymers and fluorinated photoacid generators (PAG) as model systems to study the material properties of resists that contribute to LER.

In previous work on these systems, it was shown that PAG is a major material contributor to the surface roughness of partially developed samples.[1] Depth profiling of samples after 248 nm exposure and post-exposure bake revealed that the innate material roughness of the resist varied periodically with the amount of material removed.[2] This periodicity was not seen in unexposed model resists that were constructed with acrylic acid replacing some of the tert-butylacrylate to mimic the deprotection reaction in the resist.   We have also developed a method to use an exposure curve on a single wafer to mimic the depth profiling curves and shown that the two methods are equivalent.[3]

Chemical force microscopy (CFM), also known as functionalized atomic force microscopy or f-AFM, is a variant of AFM that is capable of measuring chemical differences on a surface with high spatial resolution.[4] In CFM, the AFM tip

---

is functionalized with a specific chemistry with the goal of having the tip interact differently with different chemistries on the sample.[5] CFM, is therefore, capable of measuring chemical heterogeneities in photoresist at length scales relevant to the needs of future lithographic processes.[6]

As our previous experiments have led us to speculate that chemical segregation of resist components is contributing to the innate material roughness of these resists, we have applied CFM to our model resists to better understand how component segregation influences innate material roughness and hence LER.

2. METHODOLOGY

2.1. Model resists

Model resists were formulated with poly(hydroxystyrene-co-styrene-co-t-butylacrylate-co-acrylic acid) obtained from DuPont Electronic Polymers. Di(t-butylphenyl)iodonium perfluorobutanesulfonate (DTBPI-PFBS) or triphenylsulfonium perfluorobutanesulfonate (TPS-PFBS) were obtained from Toyo Gosei. Tertbutyl ammonium hydroxide (TBAH) was obtained from Aldrich Chemical.

All samples were spun on silicon wafers to a thickness of 250 nm. All exposures were with a Canon EX-4 248-nm 0.6NA stepper. Post exposure bake (PEB) was at either 100°C or 130°C for 60 s. Samples were developed in 0.26N tetramethylammonium hydroxide for 40 s.

Samples consisted of four unexposed samples and four samples with a dose series from 0.1 mJ/cm^2 to 22.4 mJ/cm^2 in 0.1 mJ/cm^2 steps. The unexposed samples consist of two samples of 66:20:10:4 HOST:Styrene:TBA:AA (Polymer K1) coated to 260 nm. One sample was left undeveloped and one sample partially developed to leave a 149 nm thick film. The remaining two unexposed samples consist of the same polymer with 5% DTBPI-PFBS (LUVR-99205-10) coated to 245 nm. One sample was left undeveloped and one sample partially developed to leave a 142 nm thick film. The dose series samples consisted of two samples of 65:20:15 HOST:Styrene:TBA with 5% DTBPI-PFBS and 0.38% TBAH (LUVR-99203), one with a PEB at 100°C and the other at 130°C, and two samples of 65:20:15 HOST:Styrene:TBA with 5% TPS-PFBS and 0.38% TBAH (LUVR-99258), one with a PEB at 100°C and the other at 130°C.
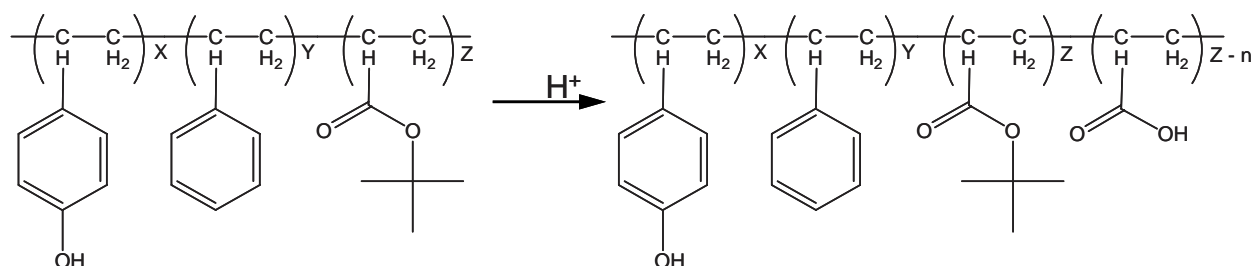
Figure 1: Chemical structures of starting and partially deprotected polymer. The starting terpolymer for the exposed samples was Polymer J (X=65, Y=20, Z=15). For the unexposed samples we used Polymer K1 (X=66, Y=20, Z=10, Z-n=4).

2.2. Chemical force microscopy

Chemical force microscopy was performed using an Asylum Research MFP-3D atomic force microscope. The AFM was operated in lateral force mode using a methyl functionalized AFM tip. AFM tips were functionalized either by 1) starting with a gold coated AFM tip (Olympus, OMCL-RC800PB1), UV cleaning and soaking in ethanol for 15 min followed by incubation for 18 h in an 0.1 mmol/L solution of octadecanethiol in ethanol[7] or 2) starting with a silicon AFM tip (MicroMasch, CSC38/AIBS), UV cleaning and incubating for 10 min in a freshly prepared 25 mmol/L solution of octadecyl trichlorosilane in anhydrous toluene. Samples were placed in a closed fluid cell and purged with dry nitrogen for a minimum of 18 hours to remove any bulk water from the sample and eliminate the effects that variable humidity can have on lateral force images. Topography and lateral force images were simultaneously collected. Both the left-to-right and right-to-left scan directions were captured.

Image analysis was performed using the MFP-3D software (Asylum Research) on an Igor (Wavemetrics) platform. The RMS roughness was calculated after flattening and plane fitting the images. With any RMS roughness measurement taken by AFM, it should be noted that the finite size of the AFM tip will prevent the tip from reaching the bottom of narrow features. The chemical force images were taken as the difference between the lateral force images in the two scan directions. We found that the two scan directions were typically offset by several pixels. To correct for this we used the ImageRegistration function in Igor to find the horizontal offset between the topography images from the two scan directions and then applied this offset to the lateral force images. The chemical force data is not calibrated and is expressed in units of deflection as measured by the voltage difference in the split photodiode of the AFM. While the units are arbitrary, the zero is a true zero point indicating no difference in deflection between the two scan directions. Additionally, if no adjustments are made to the tip or alignments of the AFM, then a series of images contain comparable data.

3. RESULTS AND DISCUSSION

3.1. Unexposed samples

Figure 2 shows representative AFM topography images of the unexposed samples of Poly-K1 undeveloped (a) and partially developed (b), and LUVR-99205 undeveloped (c) and partially developed (d). The corresponding chemical force images are shown in Figure 1e-h. The surfaces of the undeveloped samples of the Poly-K1 with and without the PAG are smooth with an RMS roughness of 0.32 nm and 0.35 nm respectively over a one square micron area. There is also little contrast in the chemical force images indicating a relatively uniform surface chemistry. The partially developed samples are significantly rougher. The RMS roughness of the partially developed Poly-K1 sample is 1.2 nm. In the chemical force image there are scattered areas of higher friction ranging from 10 nm to 200 nm in lateral dimension and covering 6% of the surface. These regions have 50% higher friction (6.0 mV vs. 3.9 mV) than the background. The background friction is equal to that found on the undeveloped Poly-K1 sample (3.8 mV). The partially developed LUVR-99205 sample has an RMS roughness of 2.5 nm. The chemical force image shows a bimodal distribution with 28% of the surface having a friction signal of 5.8 mV, nearly twice the background of 3.1 mV. The friction of the undeveloped LUVR-99205 sample is 3.4 mV.
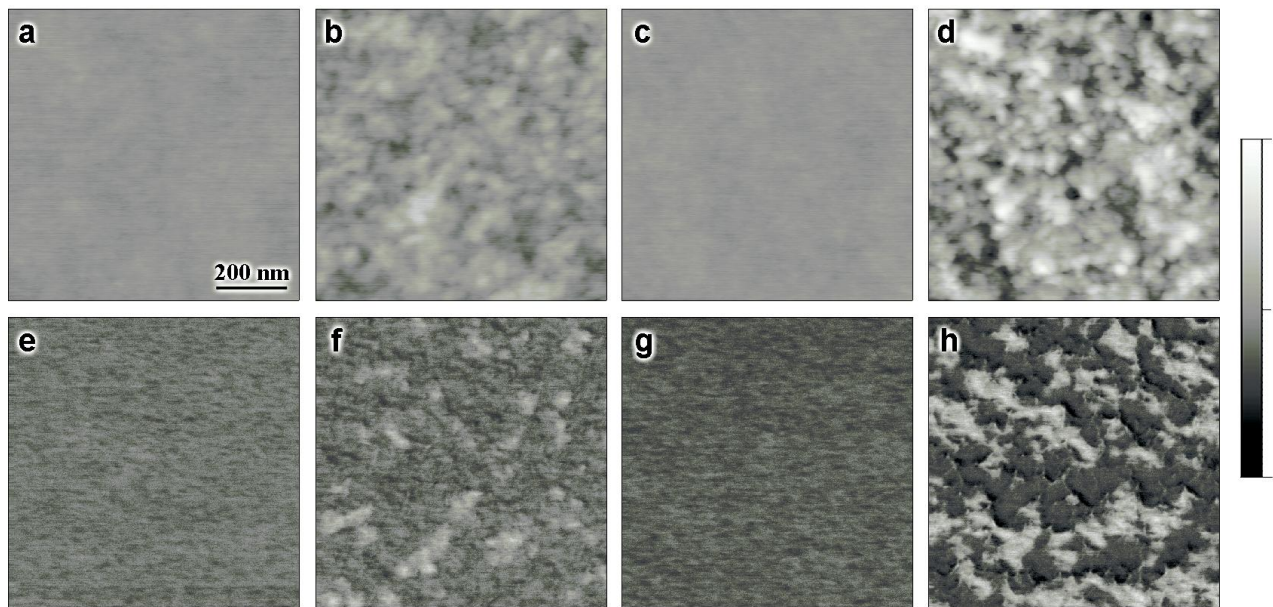
Figure 2: Topography (a-d) and chemical force (e-h) AFM images of unexposed model resists: undeveloped Poly-K1 (a, e), partially developed Poly-K1 (b, f), undeveloped Poly-K1 with 5% PAG (c, g), and partially developed Poly-K1 with 5% PAG (d, h). The z-scale for the topography images is 20 nm black to white, and for the chemical force images is 0 mV (black) to 10 mV (white).

The low chemical contrast and similar chemical force of the undeveloped images indicates that the addition of the PAG does not significantly change the surface interaction with the methyl terminated AFM tip and that both surfaces have a uniform chemistry. The slight contrast in the partially developed Poly-K1 sample may indicate that there is some tendency for the hydrophobic and hydrophilic groups in the polymer to segregate either when the film is prepared or during development. The partially developed LUVR-99205 sample shows a strong chemical contrast between different regions on the surface indicating a segregation of the PAG from polymer. Again, this may occur during the film preparation or it may be the result of the developer preferentially dissolving the polymer and leaving the less soluble PAG to aggregate on the resist surface. As the PAG aggregates, it will inhibit further dissolution. We believe this segregation contributes to the increased surface roughness as regions with different PAG concentration develop at different rates.
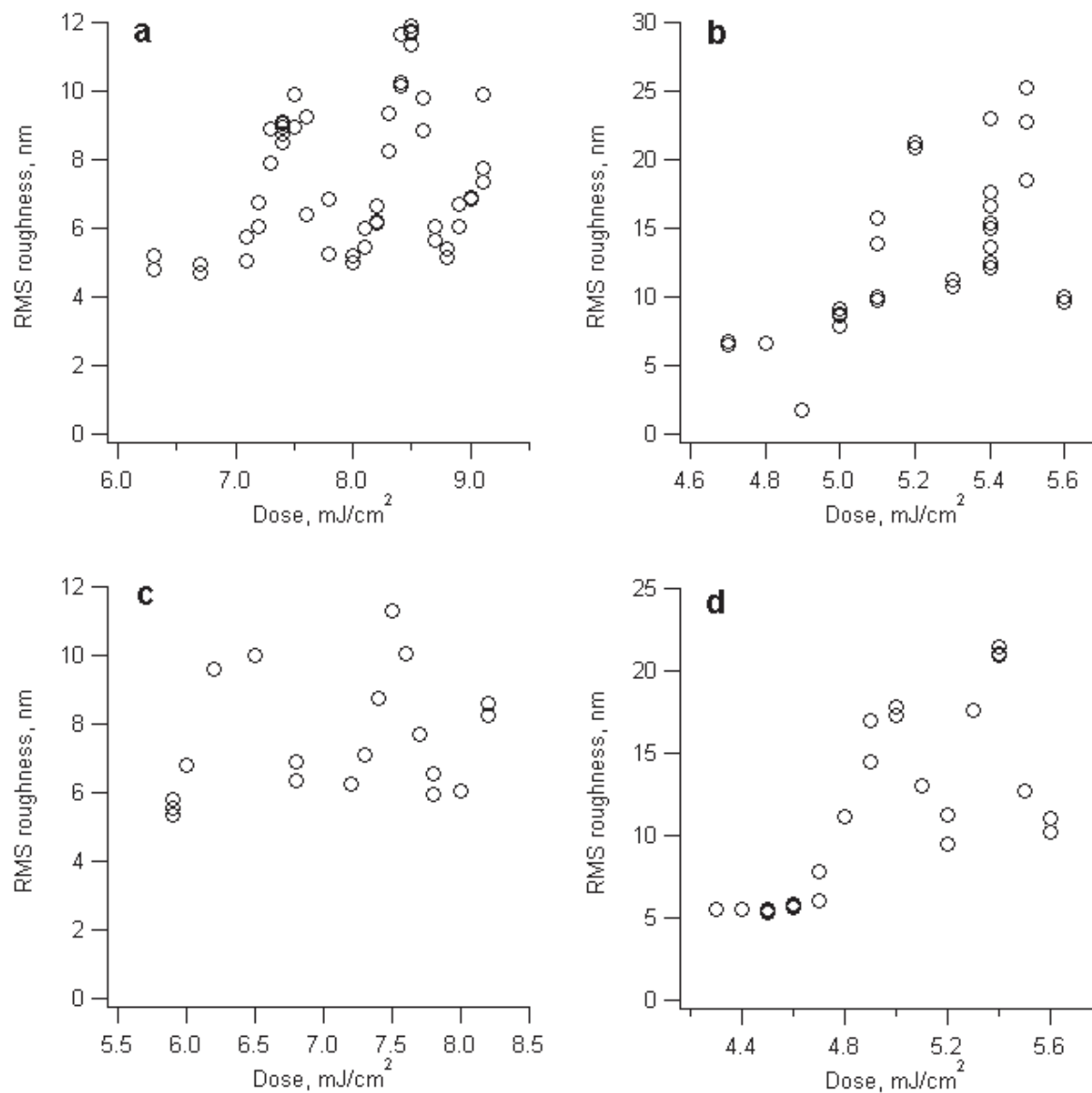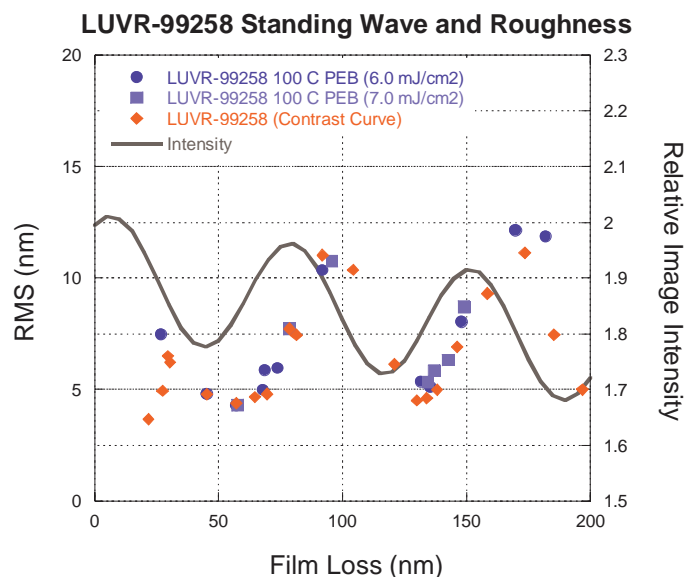

Figure 3: RMS roughness as a function of dose for LUVR-99203 with PEB 100°C (a), LUVR-99203 with PEB 130°C (b), LUVR-99258 with PEB 100°C (c), and LUVR-99258 with PEB 130°C (d). In this scheme higher doses correspond to greater film loss during development. All four samples show a series of maxima and minima in the RMS roughness with significantly higher maxima for the 130°C PEB samples.

3.2. Exposed samples

AFM images of the dose exposure series were taken of the partially developed LUVR-99203 and LUVR-99258 samples. Topography images were analyzed for their RMS roughness as a function of dose and the results are plotted in Figure 3. All four samples show an oscillatory behavior of the roughness with dose with the RMS peaking at least twice through the contrast curve as has been previously seen in our depth profiling experiments.[2] The resists all have a baseline RMS of about 5 nm. For the 100°C PEB samples, the peaks are twice the baseline value of the RMS. For the 130°C PEB samples, the RMS roughness increases to 5 times the baseline value.

We calculated the radiation intensity that we would expect in the resist during a 248 nm exposure and find a standing wave with a 10% intensity variation. A plot of the intensity vs. depth and the roughness vs. depth are shown in Figure 4. The periodicity of the surface RMS roughness was equal to, but out of phase with, that of the standing wave of the 248 nm exposure in the resist. Based on this, we speculate that the variation in the exposure intensity drives component segregation during the PEB, leading to the periodicity in the surface roughness as material is removed during development.

Figure 4: Comparison of depth profiling of RMS roughness with RMS roughness determined from a single contrast curve for LUVR-99258 (left scale) and a plot of the calculated exposure intensity as a function of depth in the resist (right scale).

Topographic images of the samples show a similar evolution of the surface of both resists at both PEB temperatures. Figure 5 shows AFM topography images from a series of doses for the LUVR-99258 with a PEB of 130°C. At low doses, the resist has a nodular structure with the RMS roughness dominated by the gaps between nodules, while the tops of the nodules remain relatively equal in height indicating an even dissolution rate across the film. As the RMS roughness of the resist increases, holes of the size of the nodules appear in the surface. The peak in the roughness occurs when approximately half the nodules have dissolved (c). The nodules continue to dissolve until there is a new smooth surface with only a few undissolved nodules on top and only few nodules dissolved from the next layer (d). The process repeats as the roughness increases until about half of the next layer of nodules is removed (e) and smoothens as the last of the layer dissolves and the next layer is just beginning (f). This indicates that there are planes within the film that are much less soluble than the bulk. The process of dissolution is somewhat analogous to the geologic process of mesa formation where an insoluble layer of rock protects the more soluble layers underneath it, but once the capping layer is removed the soluble layers quickly erode until the next insoluble layer is reached.
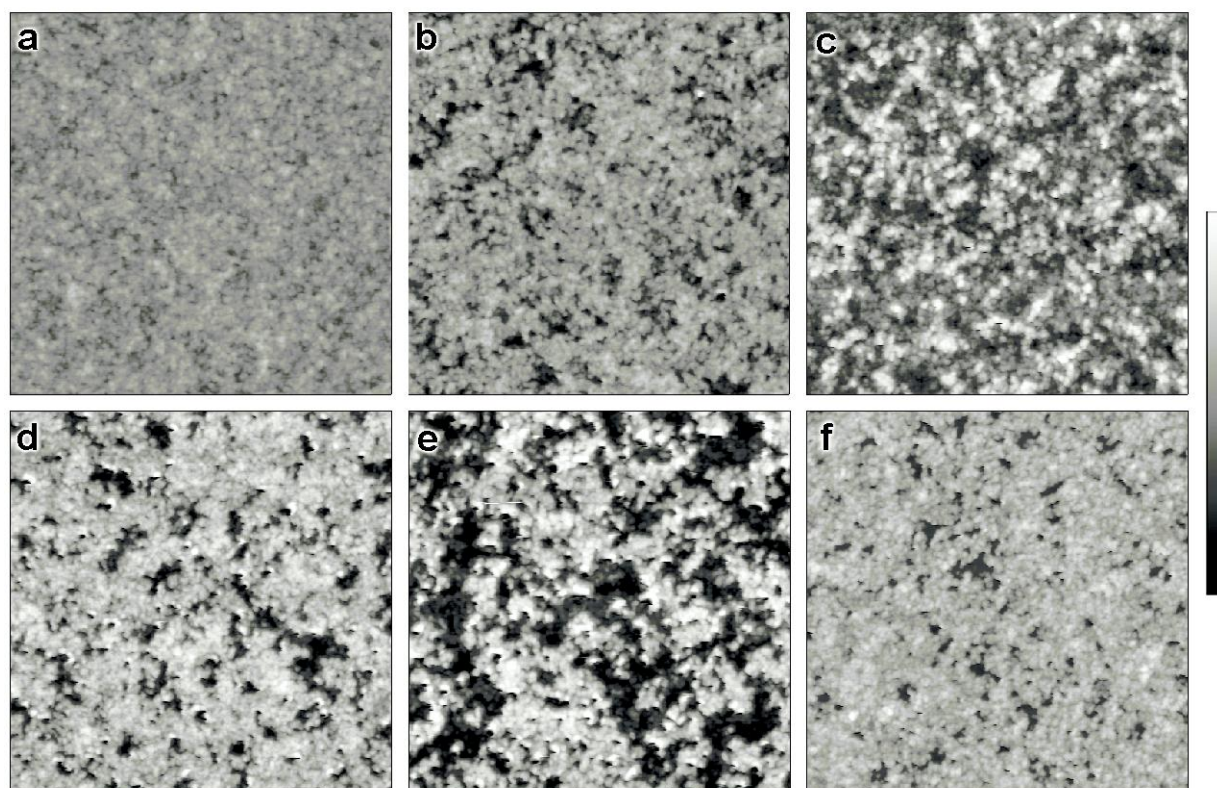
Figure 5: AFM images of partially developed LUVR-99258 with a 130°C PEB at a series of different exposures corresponding to different depths in the resist. The exposures increase by 0.2 mJ/cm^2 starting at 4.6 mJ/cm^2 in (a) and ending at 5.6 mJ/cm^2 in (f). Images (c) and (e) correspond to maxima in the RMS roughness and the others are near the minima. See Figure 3d for the corresponding RMS roughness vs. dose plot. All images are 5 micron by 5 microns and the z scale is 100 nm black to white.

Chemical force images of the partially developed surfaces show several distinctive features. The boundaries of the nodules appear highlighted by high friction lines. This is likely an artifact of the tip contacting the two nodules at the same time. The nodules themselves display differing amounts of friction corresponding to differences in the surface chemistry. However, the contrast between the nodules is significantly less than that seen in unexposed, partially developed Poly-K1 with 5% PAG. Figure 6 shows a comparison of topography and chemical force images taken on the 6.7 mJ/cm^2 exposure (a,c) and the 7.4 mJ/cm^2 exposure (b,d) of the LUVR-99203 resist with 100°C PEB. The 6.7 mJ/cm^2 exposure has a low RMS roughness while the 7.4 mJ/cm^2 exposure is from near a peak in the RMS roughness. Despite this, the chemical force images of the two samples are quite similar. This indicates either that the surfaces are chemically similar or that the methyl terminated tip is not sensitive to the chemical differences. It is possible that while the tip is clearly sensitive to the PAG in the unexposed samples, the tip is not sensitive to the dissociated PAG in the exposed samples. It is also possible that the difference in dissolution rates is so great that we are always imaging a surface with a high PAG content and rarely "catch" a soluble surface before it disappears. Similar results were obtained for the other three exposed samples.
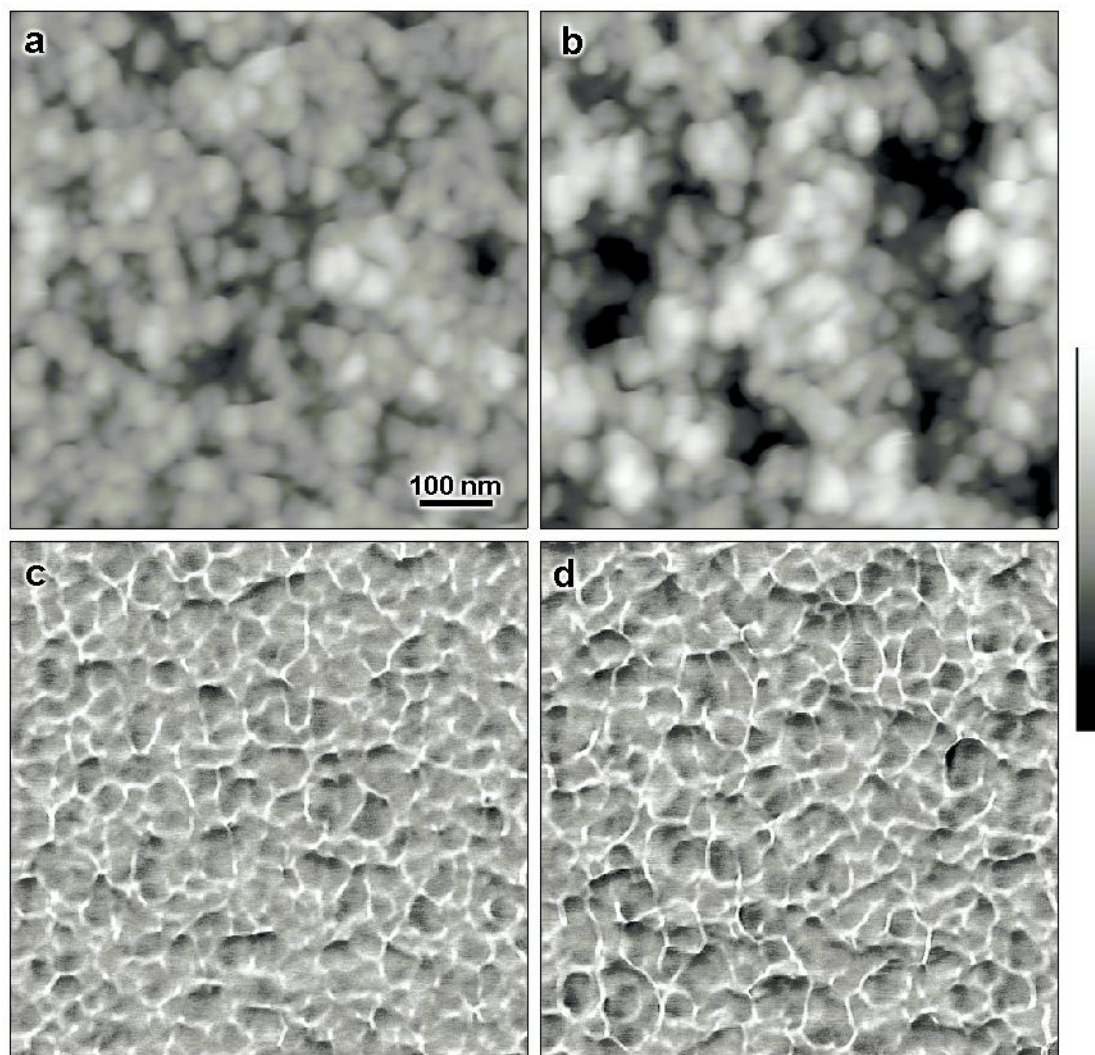
Figure 6: AFM topography (a, b) and chemical force (c, d) images of LUVR-99203 exposed at 6.7 mJ/cm^2 (a, c) and 7.4 mJ/cm^2 (b, d). The 6.7 mJ/cm^2 exposure yields a low RMS roughness and the 7.4 mJ/cm^2 exposure a high RMS roughness. See Figure 3a for the corresponding RMS roughness vs. dose plot. The z-scale for (a) and (b) is 50 nm black to white.

4. CONCLUSIONS

We have imaged with AFM dose series of ESCAP type model resists and found a periodic variation in the surface RMS roughness that is consistent with previous results found via depth profiling. The AFM images show that in unexposed resists and in the early stages of development in exposed resists that have been post-exposure baked, the roughness is caused by the formation of nodules separated by narrow crevasses on the resist surface. Beyond the early stages, the exposed resists develop by the removal of nodules in layers. The roughness peaks as half of a layer is removed, then falls as the layer finishes and the next layer begins. The periodicity of the layers is the same as the periodicity of the standing wave of the 248 nm exposure radiation leading us to conclude that variation in exposure intensity causes the initial chemical heterogeneity in the sample. The increase in the peak RMS roughness with elevated PEB temperature indicates that the diffusion of species in the resist during PEB tends to enhance the chemical segregation rather than blur out the initial differences caused by the standing wave.

Chemical force microscopy revealed a strong chemical heterogeneity on the surface of a partially developed sample of unexposed resist containing PAG compared to a comparable sample with no PAG. The PAG-containing sample has a

significantly higher innate material roughness than that without PAG leading us to conclude that the chemical heterogeneity implies a difference in dissolution rates which drives increased roughness. On the exposed samples we see some chemical difference, but not the strong contrast we see on the unexposed samples.

5. ACKNOWLEDGEMENTS

6. REFERENCES

1. Fedynyshyn, T. H., Pottebaum, I., Astolfi, D. K., Cabral, A., Roberts, J., and Meagley, R., "Contribution of Photoacid Generator to Material Roughness" Journal of Vacuum Science and Technology B **24**, 3031-3039, 2006.

2. Fedynyshyn, T. H., Sinta, R. F., Astolfi, D. K., Cabral, A., Robert, J., and Meagley, R., "Deconstructing the Resist to Probe Innate Material Roughness" Proceeding of SPIE **6153**, 615315, 2006.

3. Fedynyshyn, T. H., Astolfi, D. K., Cabral, A., and Roberts, J., "PAG Segregation During Exposure Affecting Innate Material Roughness" Proceeding of SPIE **6519**, 2007.

4. Frisbie, C. D., Rozsnyai, L. F., Noy, A., Wrighton, M. S., and Lieber, C. M., "Functional Group Imaging by Chemical Force Microscopy" Science **265**, 2071-2074, 1994.

5. Noy, A., Frisbie, C. D., Rozsnyai, L. F., Wrighton, M. S., and Lieber, C. M., "Chemical Force Microscopy: Exploiting Chemically-Modified Tips to Quantify Adhesion, Friction and Functional Group Distributions in Molecular Assemblies" Journal of the American Chemical Society **117**, 7943-7951, 1995.

6. Woodward, J. T. and Solak, H. H., "Chemical Force Microscopy of 30 nm Half-Pitch Latent Images in Poly(Methyl-Methacrylate)" To be published.

7. Woodward, J. T., Walker, M. L., Meuse, C. W., Vanderah, D. J., Poirier, G. E., and Plant, A. L., "Effect of an Oxidized Gold Substrate on Alkanethiol Self-Assembly" Langmuir **16**, 5347-5353, 2000.